

# YALE PEABODY MUSEUM

P.O. BOX 208118 | NEW HAVEN CT 06520-8118 USA | PEABODY.YALE. EDU

## JOURNAL OF MARINE RESEARCH

The *Journal of Marine Research*, one of the oldest journals in American marine science, published important peer-reviewed original research on a broad array of topics in physical, biological, and chemical oceanography vital to the academic oceanographic community in the long and rich tradition of the Sears Foundation for Marine Research at Yale University.

An archive of all issues from 1937 to 2021 (Volume 1–79) are available through EliScholar, a digital platform for scholarly publishing provided by Yale University Library at <https://elischolar.library.yale.edu/>.

Requests for permission to clear rights for use of this content should be directed to the authors, their estates, or other representatives. The *Journal of Marine Research* has no contact information beyond the affiliations listed in the published articles. We ask that you provide attribution to the *Journal of Marine Research*.

Yale University provides access to these materials for educational and research purposes only. Copyright or other proprietary rights to content contained in this document may be held by individuals or entities other than, or in addition to, Yale University. You are solely responsible for determining the ownership of the copyright, and for obtaining permission for your intended use. Yale University makes no warranty that your distribution, reproduction, or other use of these materials will not infringe the rights of third parties.



This work is licensed under a Creative Commons Attribution-NonCommercial-ShareAlike 4.0 International License.  
<https://creativecommons.org/licenses/by-nc-sa/4.0/>



## Field measurements of the fluid and sediment-dynamic environment of a benthic deposit feeder

by Douglas C. Miller<sup>1,2</sup> and Richard W. Sternberg<sup>1</sup>

### ABSTRACT

Field measurements of flow and sediment transport at an intertidal site in False Bay, San Juan Island, Washington, U.S.A., revealed an environment dominated by wind wave-generated oscillatory flows and discrete sediment suspension events. Time series data showed that within a few tenths of a second, near-bottom suspended sediment concentrations can rise to  $10 \text{ g l}^{-1}$ . These rapid erosion events are correlated with peak wave velocities and are followed by a more gradual (tens of seconds) decline in sediment concentration due to settling and advection. Large suspension events mixed detectable quantities of sediment to a height of 20 cm above the bottom. Flow and sediment transport rates are controlled by local weather and vary on time scales ranging from that of individual waves to that of atmospheric storm systems and seasonal changes in weather patterns. Advection of sediment can exceed individual deposit feeding rates by a factor of  $10^3$ – $10^4$ . An empirical relationship developed from weather records, together with previously published observations of detrital transport, suggests that sediment transport is rarely small enough in magnitude to be ignored as a source of food particles for surface deposit- and suspension-feeding spionid polychaetes like *Pseudopolydora kempii japonica*.

### 1. Introduction

Theoretical (Miller *et al.*, 1984), laboratory (Taghon *et al.*, 1980, 1984; Dauer *et al.*, 1981; Dauer, 1983, 1985; Miller and Jumars, 1986), and field (Jumars and Self, 1986) studies reveal that many benthic organisms and, in particular, deposit feeders are sensitive to particle transport phenomena. Miller *et al.* (1984) argue, and Miller and Jumars (1986) show, that deposit feeders are responsive to new particles moving into, as well as fecal material moving out of, an individual's feeding area. Sediment transport studies relevant to such biological processes are generally lacking, however.

There are two principal issues raised by previous work on the interaction between deposit feeding and sediment movement. The first is the magnitude of the biological sediment processing rates (principally feeding) relative to that of geophysical processing rates in, for example, units of volume of sediments moved per unit time. To date, there is but one study (Grant, 1983) comparing the two rates in a bulk, community-level manner. Grant (1983) finds that geophysical net sediment transport rates far

1. School of Oceanography, WB-10, University of Washington, Seattle, Washington, 98195, U.S.A.

2. Present address: College of Marine Studies, University of Delaware, Lewes, Delaware, 19958, U.S.A.

exceed biological processing rates on an intertidal sandflat. This implies that virtually all surficial sediment and detrital particles have been deposited there by the action of the flow rather than by defecation of a given deposit feeder (Miller *et al.*, 1984). Hence food availability is determined by production and consumption of organic matter some distance away and upstream. Conversely, microbial gardening (fostering local microbial growth for consumption as food, Hylleberg, 1975) is not a viable feeding strategy for surface deposit feeders in sedimentologically active environments. The second issue, raised by the laboratory findings of Miller and Jumars (1986), is the frequency with which sediments and fecal pellets are moved. They found that the feeding rate of a deposit feeding spionid polychaete, *Pseudopolydora kempji japonica* (Imajima and Hartman, 1964), was decreased by the accumulation of fecal material within the feeding area. Significant depression of feeding rate occurs within 2 hours if pellets are not removed.

The dependence of deposit-feeding rate on frequency of sediment (and fecal pellet) movement has serious implications for modeling of the effects of sediment transport on deposit feeders and for future attempts at laboratory simulation of field environments. It suggests that the equilibrium, steady-state approach initially applied by Miller *et al.* (1984) may be of limited utility unless sediment transport occurs (a) so frequently that food supply and fecal removal rarely limit deposit-feeding rate, or (b) so infrequently that feeding rate is controlled by other processes. While feeding rate can be measured easily in the seawater tables, and sediment transport conditions can be imposed on experimental organisms in laboratory flumes, extrapolation of results to the field is problematic. We have no knowledge of sediment supply rates in the field on biologically-important time and space scales.

The objective of our experimental work and the goal of this paper is to provide first estimates of the ecologically-relevant sediment transport rates. To place bounds on the rates and frequency of sediment transport for one species of deposit feeder in one environment, we undertook a field measurement program aimed explicitly at temporal and spatial scales relevant to individual deposit feeders. False Bay, San Juan Island, Washington, was selected as the locality because of the general background information available on its biota (Hobson, 1967; Pamatmat, 1966, 1968; Hylleberg, 1975; Brenchley, 1981; Jumars *et al.*, 1982; Wilson, 1981, 1982, 1984; Price and Hylleberg, 1982; Miller, 1984) and specifically because it was the collection site for the *P. kempji japonica* individuals used in recent laboratory studies (Jumars and Self, 1986; Miller and Jumars, 1986) that demonstrate dependence of deposit-feeding rate on sediment transport rate and frequency. The sediment transport technology that we used (Downing *et al.*, 1981; Hanes and Huntley, 1986; Beach and Sternberg, 1988) permitted us to measure transport parameters on centimeter and tenths of a second space and time scales.

The field measurements achieved in this study suggest that transport during the autumn period of measurement varied between a roughly equal balance between

ingestion rates and sediment transport rates to conditions in which sediment transport rates exceeded feeding rates by a factor of  $10^3$  to  $10^4$ . Flow is dominantly oscillatory, and sediment transport occurs in discrete suspension events in response to individual surface waves which are generated by winds in the adjacent Strait of Juan de Fuca. Thus, local weather exerts a significant control on sediment transport at False Bay. Examination of climatological weather records suggests that winds determine sediment transport rates at False Bay throughout the year. When considering the low levels of detrital transport that occur as the tide leaves and returns (Anderson, 1980; Anderson and Mayer, 1984; Wissmar and Simenstad, 1985), sediment transport appears to be of sufficient frequency and magnitude to influence deposit feeding throughout the year.

## 2. Methods

*a. Site description and field measurements.* False Bay is a circular bay, 1 km in diameter, on the west side of San Juan Island, northwestern Washington, U.S.A. ( $48^{\circ} 29' N$ ;  $123^{\circ} 04' W$ , Fig. 1). It is an intertidal sandflat that is almost completely drained on low tides below the mean low water level. It is fed by only three small streams around its perimeter, and the narrow mouth (500 m wide, depth  $-0.8$  m relative to mean low water, MLW) opens southwestwardly to the Strait of Juan de Fuca. An aerial photograph, map with bathymetry, and sediment grain size distributions are presented in Pamatmat (1966, 1968). Tides are mixed, mainly diurnal (Parker, 1977) with a diurnal range of 2.2 m and extreme highs and lows of  $+2.5$  m to  $-0.8$  m for 1984 (NOAA, 1983, based on predictions for Kanaka Bay, 0.6 km northwest of False Bay along the west side of San Juan Island). The dominant physical energy source for the bay is that of waves generated in the Strait of Juan de Fuca and which diffract, refract, and shoal into the bay. The significance of this energy is indicated by the types of large and small bedforms found there. For example, aerial photographs at low tide show a concentric arrangement of bars, typically 100 m long, 20 m wide, and up to 50 cm high. Superimposed on these bars were wave-formed, vortex (Sleath, 1984) or "cat's back" ripples, usually 8–10 cm long and 1–1.5 cm high, occasionally exhibiting an on- or offshore asymmetry. In the upper regions around the perimeter of the bay, scattered rocks are found in pools between bars.

Anecdotal evidence suggests that the relative rates of biological and physical processing of sediment vary with time and location within the bay. High in the intertidal at False Bay, fecal mounds produced by the subsurface-feeding, arenicolid polychaete *Abarenicola pacifica* (Healy and Wells) are conspicuous at low tide. During periods of calm weather, mounds persist over many tidal cycles and become quite large. However, just after tidal emersion during stormy weather, no mounds are visible. Mounds appear and grow throughout the time the flat is exposed during low tide, but are apparently dispersed during the next period of high water. We have made

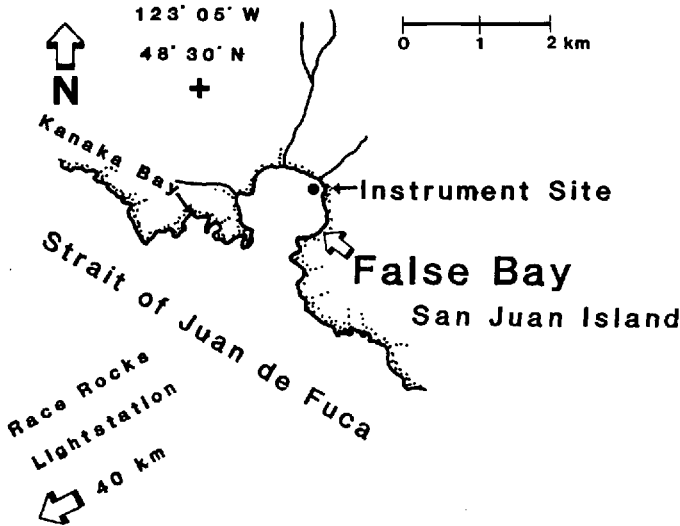


Figure 1. Location map showing instrument array site in False Bay.

similar observations on the accumulation of fecal pellets of the deposit-feeding spionid polychaete *Pseudopolydora kempii japonica* (Miller and Jumars, 1986).

At False Bay, we used an instrument system designed for making simultaneous flow and sediment transport measurements in the surf zone (Downing *et al.*, 1981; see Fig. 2; and similar to that used by Hanes and Huntley, 1986). Between 25–28 October 1984, instruments were deployed at a +1.3 m above MLW site in the northeastern sector of the bay, about 120 m from shore (Fig. 1). The site was on the crest of a low bar (about 10 cm high), 30 m inshore of the nearest pool (bar trough) at low tide. The sediment surface was fine sand (143  $\mu\text{m}$  median grain size, 86% sand by weight, sorting coefficient 1.0 phi units) covered with symmetrical wave-formed, cat's back ripples. Scattered rocks outcropped at the seaward edge of the pool. The sensors were cantilevered from two galvanized pipes pounded into the sediment, 1 m apart, on a line parallel with the crests of the wave-formed ripples (shown schematically in Fig. 2). On one pipe we mounted two Marsh-McBirney electromagnetic current meters to measure the alongshore (height above bed, 30 cm) and shorenormal (15 cm) velocity components; additionally, each meter recorded a vertical velocity component. To allow us to locate the instruments at night or when water covered the site, a marker pole with 20-cm high fluorescent orange and white bands was also attached to this pipe.

On the second pipe (one meter to the right, facing offshore) were mounted a pressure sensor and an optical backscatter suspended-sediment sensor array. Individual suspended-sediment sensors were at heights of 3.5, 6.5, 9.4, 14.7, and 19.8 cm above the bed, cantilevered out from the supporting pole. We periodically checked the instrument array and never found any indication of scour beneath the sensor array. The operation and design of this instrumentation system is described by Downing *et al.*

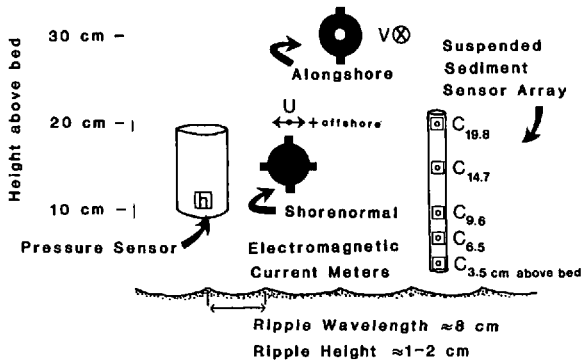


Figure 2. Schematic of instrument array showing sensor heights, measured quantities, and variable symbols. Shorenormal velocity is positive offshore (to the right). Alongshore velocity vector is perpendicular to the plane of the figure; positive direction is away from the reader. Sensor heights are drawn accurately; lateral positions have been compressed for clarity. See text for precise location of each instrument.

(1981). Data from the instruments were cabled to shore where they were recorded periodically by computer yielding a total of 50 separate runs, each 9.4 min long (5632 points at 10 Hz) and 40 min apart during a tidal cycle. This sampling scheme was designed to record conditions over a range of tidal heights and weather conditions during 4 days from 25–28 October 1984.

Data were uploaded to a mainframe computer and converted to instrument output in volts. Calibration equations for all sensors to convert from recorded voltage to scientific units are available in an appendix to Miller's (1985) dissertation. Voltages from the current meters were converted to velocities using the calibration in Downing (1983). Pressure sensor output was converted to depth using a calibration provided by R. Johnson (pers. comm.,  $r^2 > 0.999$ ,  $n = 11$ ). Suspended sediment concentrations were determined from an empirical calibration with sediment from the instrument site (R. Beach and D. Miller, unpublished; see Downing [1983] for details of the calibration procedure). Concentrations are linearly related to output voltage for each of the 5 sensors ( $r^2 > 0.997$ ,  $n = 11$ ). To allow for day-to-day differences in water clarity due to suspension of very fine silt, daily corrections based on the clearest-water run were applied to the raw concentration data for each sensor in the array (see also Hanes and Huntley, 1986). This was done as follows: the raw concentration (from each sensor) during the run with the lowest mean, uncorrected sediment concentration (as measured by the lowest sensor) on each day was subtracted from all concentrations for the day to yield an adjusted value for each sensor. These corrections were typically less than  $1 \text{ g l}^{-1}$ .

*b. Descriptive statistics and flux calculation.* We computed the mean, variance, minimum, maximum, and linear trend through time for each measured variable.

Smoothed estimates of the wave amplitude spectra were computed for the pressure sensor time series after removal of the mean and linear trend, and tapering of the ends of the time series. Although the pressure sensor was at a fixed height (10 cm) above the bottom, and therefore at variable depth (up to 1.3 m), no adjustment was made for attenuation of high frequency wave components. Total wave energy was proportional by a factor of  $\rho g/2$  (where  $\rho$  is the fluid density and  $g$  is the acceleration of gravity) to the integral of the smoothed spectrum. Wave energy and modal frequencies from smoothed spectra in 1–6 s (wind waves) and 6–30 s (ocean swell) bands were also computed. Since alongshore velocities were relatively small, all sediment flux calculations were done with the shorenormal velocity component ( $U$ ) only, and are indicated in this paper by an “X” subscript. The instantaneous horizontal sediment flux at 3.5 cm above the bottom is the product of this shorenormal velocity and the suspended sediment concentration at the lower most sensor. Velocities were measured at 15 cm above the bed and assumed to be representative of the near-bottom velocity outside the wave boundary layer, an assumption considered and verified below. We likewise assumed suspended-sediment concentrations below the bottom sensor to be equal to that at the lowest sensor, 3.5 cm above the bottom. As mean suspended sediment concentrations were observed to decrease exponentially with height above the bed from 3.5 to 19.8 cm, this assumption leads to a conservative estimate of the sediment flux near the bed. (A more detailed justification of this assumption is included in the Results and discussion section.) Thus the horizontal sediment flux multiplied by the height of the sensor (3.5 cm) gives a lower bound on the vertically-integrated, near-bottom sediment transport rate which, for convenience, we will refer to as the “near-bed” sediment transport rate.

For descriptive and comparative purposes, we calculated three mean flux values for each 9.4 minute sampling period. First, the net horizontal flux  $Q_{XNET}$  is the mean of the instantaneous horizontal flux described above. Second, the mean scalar or absolute flux  $Q_X$  is the mean of the absolute value of the instantaneous horizontal flux; it is the average flux rate without regard to direction. When mean velocities are small compared to oscillatory components and this flux is integrated vertically (as above), it is equivalent to the average bedload flux over the wave half cycle (the net transport over the full cycle being approximately zero). This is the parameter commonly used to describe sediment transport in oscillatory flows (see the summary of models in Sleath, 1984). Third, a deposition or vertical flux rate  $Q_D$  was calculated. Its calculation is based on the assumption that the difference in sediment concentration between successive samples is a measure of the amount of material eroded (or, depending on the sign of the difference, deposited) locally below the sensor in the sampling interval, or eroded (or deposited) from some point away and advected in suspension to the sensor. Further, the rate of change in concentration approximates the erosion rate averaged over the bed, assuming spatial homogeneity in sediment concentration and flow characteristics. If there is a uniform concentration at 3.5 cm above the bed and below,

the erosion (or depending on the sign of the change in concentration, deposition) rate per unit area of bed beneath the sensor is therefore the difference in successive concentration samples, divided by the sampling interval (0.1 s), times 3.5 cm (vertically integrating the concentration). The mean rate was calculated by summing all positive instantaneous rates and dividing by the number of concentration differences used in the calculation (i.e., 5631, one less than the total number of samples in a run). To eliminate instrument noise from biasing (by inflating) this estimate, a sediment-concentration difference threshold of  $0.03 \text{ g l}^{-1}$  was used; this corresponds to a unit change in the least significant bit of the 12-bit analog-digital converter. As noted above for the horizontal flux calculations, a trend of increasing sediment concentration toward the bed would imply more erosion than accounted for by the above calculation. Thus, we again may have some underestimate of the flux, and this point will be further discussed below.

*c. Meteorological and tide data.* Weather reports, including wind speed and direction, and reported wave heights for the field sampling period were obtained from unpublished data in the files of the National Weather Service Office, National Oceanic and Atmospheric Administration (NOAA) Regional Center 8 in Seattle. These files, along with published climatological data for Race Rocks Lightstation ( $48^{\circ} 18' \text{ N}$ ;  $123^{\circ} 32' \text{ W}$ , 40 km southwest of False Bay), were chosen as representative of winds and waves in the Strait of Juan de Fuca (Thomson, 1981). Reports for the field sampling period were updated every three hours; we used the weather report closest in time to each run for purposes of data analysis. Additionally, monthly wind speed-class percentages from Race Rocks for 1978–1982 were obtained from the Environment Canada Monthly Record (1978–1982). As we wished to include predicted tide heights as a predictor variable in our regression analysis of all runs, we calculated these using a least squares fit of major diurnal and semidiurnal tidal components (Parker, 1977) to tabulated high and low water predictions for Kanaka Bay (NOAA, 1983).

### 3. Results and discussion

*a. Descriptive summary of flow and sediment transport.* Data collected at False Bay over the four-day sampling period included a wide range of weather, wave, and tide conditions. All measured and calculated variables for each run are tabulated in Miller (1985). Mean wave heights over the study period ranged from 2–12.5 cm (corresponding to significant wave heights of 3–20 cm), with a mean for all runs of 6 cm. Of the wave energy, 88% was found in the 1–6 s wind wave band (typical spectrum peak period, 3.6 s), with 9.5% contributed by the swell band (6–30 s period, 8.6 s peak). Mean currents at the site varied from 1–8  $\text{cm s}^{-1}$  offshore, regardless of the stage of the tide. This unexpected feature of the local circulation was confirmed by direct observation at the instrument site. Alongshore currents averaged a few  $\text{cm s}^{-1}$  to the northwest. In all runs, flow and sediment transport (when present) were dominated by



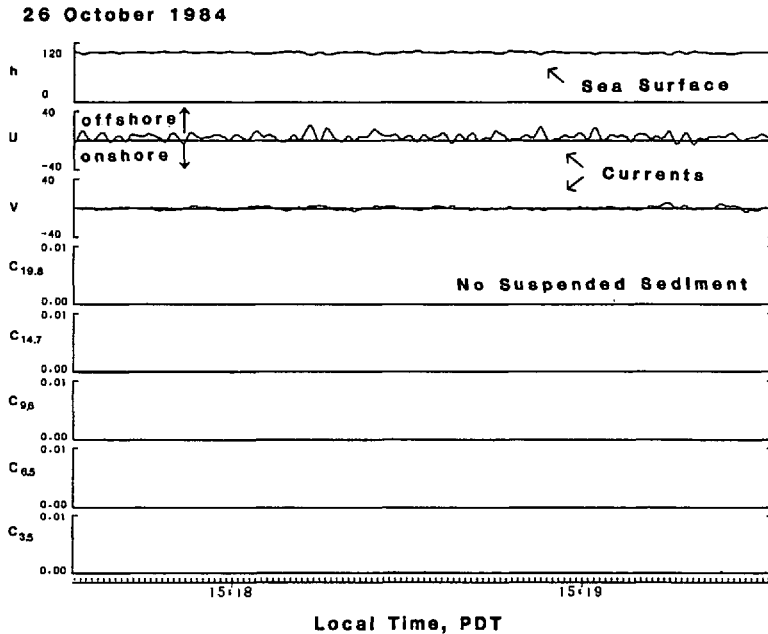


Figure 3. Two-minute excerpt of data collected during a sedimentologically quiet period at False Bay. Time series are (from top to bottom): water depth ( $h$  cm), shorenormal velocity ( $U$   $\text{cm s}^{-1}$ , positive offshore), alongshore velocity ( $V$   $\text{cm s}^{-1}$ , positive to the left facing offshore), and suspended sediment concentration ( $C$   $\text{g cm}^{-3}$ ) at 5 heights above the bottom (indicated in centimeters by subscripts). Note that  $0.01 \text{ g cm}^{-3}$  equals  $10 \text{ g l}^{-1}$ . Each tic mark on the time axis is 1 s.

wave-induced oscillatory currents. Peak wave velocities were at least equal in magnitude to the mean flow component and during energetic periods exceeded  $40 \text{ cm s}^{-1}$  at 15 cm above the bed. Suspended-sediment time series showed rapid (within a few tenths of a second) rises in concentration (by erosion or advection) correlated with peak wave velocities. Peak sediment concentrations in these suspension events reached  $10 \text{ g l}^{-1}$  at 3.5 cm above the bottom. Following large suspension events, detectable quantities of sediment were mixed to a height of 20 cm above the bottom.

Daily and hourly variations in wave height and transport intensity were evident. On 25 October high rates of suspended sediment transport in continuous suspension of sediments were evident in early afternoon runs and tapered substantially by that evening. Low levels of transport were observed on both the 26 and 27 October. Runs on the afternoon of the 26th were particularly free from even small suspension events. Moderate to high levels of sediment transport activity occurred on the 28th and were characterized by discrete suspension events associated with individual large waves or wave groups.

As specific examples of the range of flow and sediment transport conditions observed

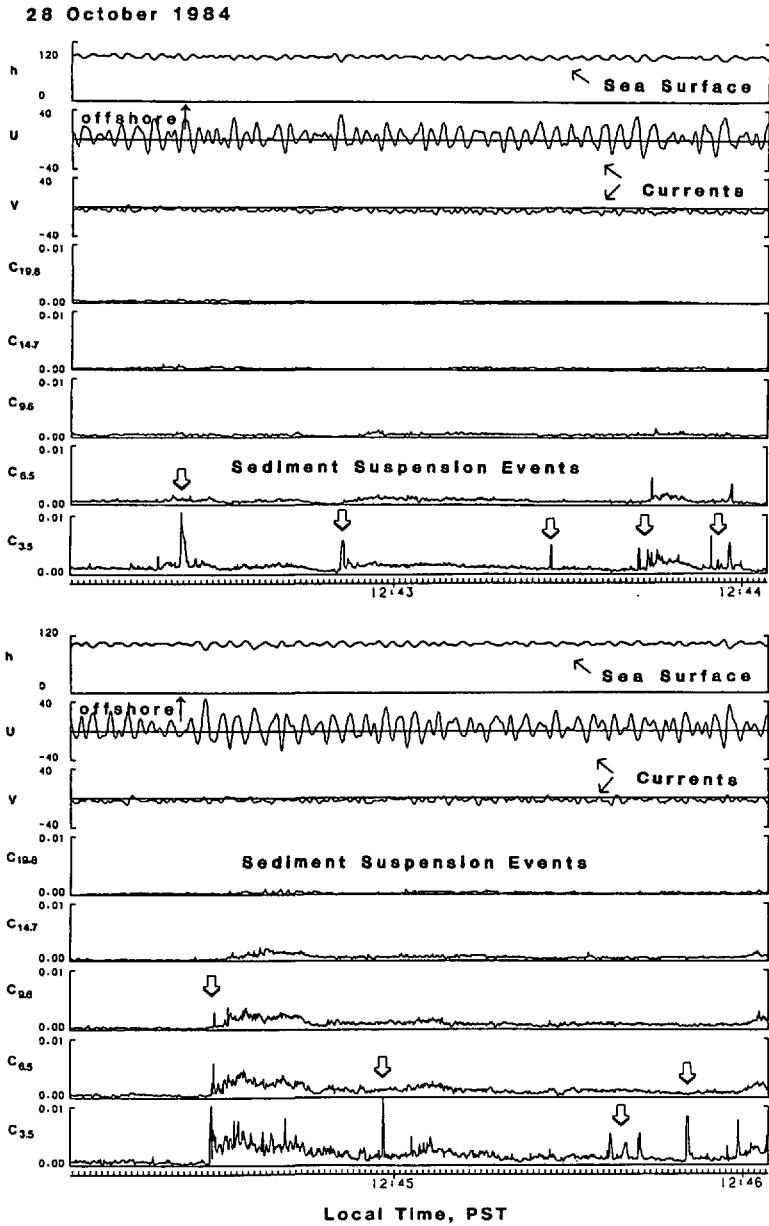


Figure 4. Two, 2-minute excerpts of data collected during a sedimentologically active period at False Bay. Arrows indicate suspension events. Explanation of time series and other symbols is given in Figure 3.

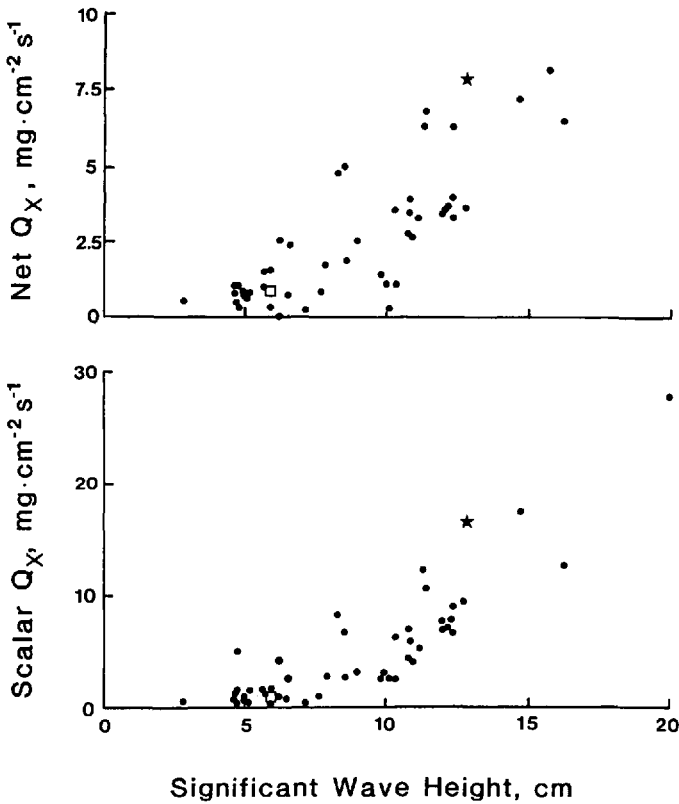


Figure 5. Mean net and scalar sediment fluxes at False Bay as a function of significant wave height,  $H_s = 2.83 \times \sqrt{(\text{integral of the pressure sensor wave spectrum in cm}^2)}$ . Average wave height is  $1.77 \times \sqrt{(\text{spectrum integral})}$ . Open square indicates data collected in the sedimentologically quiet run illustrated in Figure 3; star corresponds to the sedimentologically active run in Figure 4.

at False Bay, we present excerpts from two runs in detail. On 26 October (Fig. 3) waves of 3.7 cm mean height passed shoreward in water 111 cm deep. Only about half the total wave energy fell in the wind wave band (modal period, 3.6 s), while 45% was attributable to swell (modal period, 11.2 s). The mean offshore current was  $5 \text{ cm s}^{-1}$  and was comparable to peak wave velocities. These flows caused no movement of sediment as detected by the lowermost suspended sediment sensor.

Data collected on 28 October were dramatically different (Fig. 4). Mean wave height was 8 cm in 102 cm of water with 95% of the wave energy due to wind waves (modal period, 2.8 s). Discrete suspension events, apparent in even the highest suspended sediment sensor, were associated with 20-cm high waves and peak velocities in excess of  $40 \text{ cm s}^{-1}$ . As in other sedimentologically active runs, mean velocities are minor compared to the oscillatory components. Mean suspended sediment concentra-

Table 1. Coefficients of determination ( $r^2$ , or, equivalently, the proportion of variance explained) by predictors of sediment fluxes in False Bay, October 1984 based on a series of 50 observations. All coefficients exceed the critical value for the appropriate test of no significant regression at an  $\alpha$  level of 0.05. The proportion of wave energy variance explained by wind speed is 0.24; the proportion of velocity variance explained by wave energy is 0.94.

Predicting variables	Net transport	Scalar flux	Deposition rate
	$Q_{x\ net}$	$Q_x$	$Q_D$
Mean shorenormal velocity	0.15	0.09	0.17
Shorenormal velocity variance	0.75	0.85	0.80
Wind wave energy	0.74	0.82	0.76
Total wave energy	0.73	0.81	0.73
Wind wave energy & measured water depth	0.74	0.84	0.76
Wind speed & measured water depth	0.35	0.28	0.49
Wind speed $\times \cos((\text{wind direction}-200^\circ)/2)$	0.22	0.18	0.38
Wind speed alone	0.30	0.26	0.30
Reported wave height	0.19	0.18	0.29

tions near the bottom were often above  $1\text{ g l}^{-1}$ . Sediment at this concentration visibly clouds the water. Mean suspended sediment concentration decreased exponentially with height above the bed.

During the four days data were collected, it became apparent that local waves, more than any other single factor, determined sediment transport activity. This observation is borne out in the strong correlation between significant wave height and the net and scalar horizontal fluxes measured at False Bay ( $r^2 = 0.69$  and  $0.72$ , respectively, Fig. 5).

*b. Factors controlling sediment transport.* A linear regression analysis of sediment fluxes with a number of environmental variables is presented in Table 1. In this simple, exploratory analysis, we assume that the run data are independent observations although they in fact were collected in a proscribed sequence in each tidal period. Mean shorenormal velocity is positively related with all three sediment fluxes, but explains little (9–17%) of their variance. Thus, characterizing the flow regime at this site in False Bay with simply a single mean velocity is of little value. In contrast, the variance of the shorenormal velocity, a measure of the wave component of the velocity, explains a large fraction (75–85%) of the variance in all three transport rates. As expected from our visual observations, wind wave energy is highly related ( $r^2 = 0.74$ – $0.82$ ) with flux rates. There is only a slight, if any, improvement in flux predictions if the mean water depth calculated from the pressure sensor output is included in a multiple regression ( $r^2 = 0.74$ – $0.84$ ). Similarly, there is no additional explanatory value from including water depth predicted from tide tables in a regression with wind wave energy ( $r^2 = 0.74$ – $0.84$ , not tabulated). Wave theory (e.g., Dean and Dalrymple, 1984) suggests that near-bottom orbital velocities should increase as water column depth decreases. However, the actual relationship between orbital velocity and

depth at the experimental site in False Bay is considerably more complex than this because of diffraction at the bay mouth and refraction and wave travel over the extensive flat seaward of the instruments. For example, when water at the instrument site is shallow, waves break and dissipate energy on seaward bars and are much attenuated by the time they reach the head of the bay. At least at the instrument site near mean water level in False Bay, variations in water depth fail to substantially improve prediction of sediment fluxes.

Approximately 75% (range, 73–81%) of the variance in flux rates is explained by the single variable of total wave energy. Wave and wind reports from Race Rocks Lightstation are correlated with flux rates (lowest four rows in Table 1), but to a substantially lower degree than that of wave-related variables measured at False Bay itself (rows 2–5). Wind speed and water depth together are better predictors of fluxes than wind speed adjusted for direction of exposure of False Bay (200° from true north) or wind speed alone (7th and 8th rows, respectively). Since wave reports from Race Rocks correlate poorly with locally-measured wave energy ( $r^2 = 0.15$ , not tabulated) it is not surprising that Race Rocks wave reports correlate poorly with sediment flux rates at False Bay (last row in Table 1).

*c. Consideration of the accuracy of flux estimates.* Sediment fluxes discussed above are accurate if flow velocities measured at a height of 15 cm and if sediment concentrations measured at a height 3.5 cm are both representative of conditions near the bed, specifically at or below 3.5 above the bed. Because of the no-slip condition, fluid velocities are zero at the bed (if it is not moving). Suspended sediment concentrations increase exponentially toward the bed. The latter statement is justified by both theoretical arguments (e.g., Sleath, 1984) and from our False Bay results using mean suspended sediment concentration at heights of 3.5–19.7 cm from sedimentologically active periods on 28 October 1984. With one variable (i.e., velocity) increasing away from the bed and the other (i.e., concentration) increasing toward the bed, it is not clear how reliable an estimate can be made using the product of the variables (i.e., velocity times concentration yields a horizontal flux) measured at separate, experimentally convenient heights. To assess the accuracy of our approximation in the near-bed region, we have extended the steady-flow analysis of Muschenheim (1987) to our oscillatory flow flux estimates. For illustrations, we considered active transport conditions similar to that illustrated in Figure 4 (and denoted by stars in Figs. 5 and 6) and specifically the suspension event which occurred at 12:44:17 PDT (Fig. 4, bottom panel): a wave height of 15 cm (wave amplitude,  $a = 7.5$  cm), wave period  $T = 2.8$  s, water depth 90 cm. We used linear wave theory to calculate wave and flow characteristics such as the wavelength (767 cm) and the velocity field from the height of the electromagnetic current meter (15 cm) to the top of the wave boundary layer. The use of linear wave theory is reasonable given that the Ursell parameter for above situation is about half that value above which cnoidal theory is generally considered

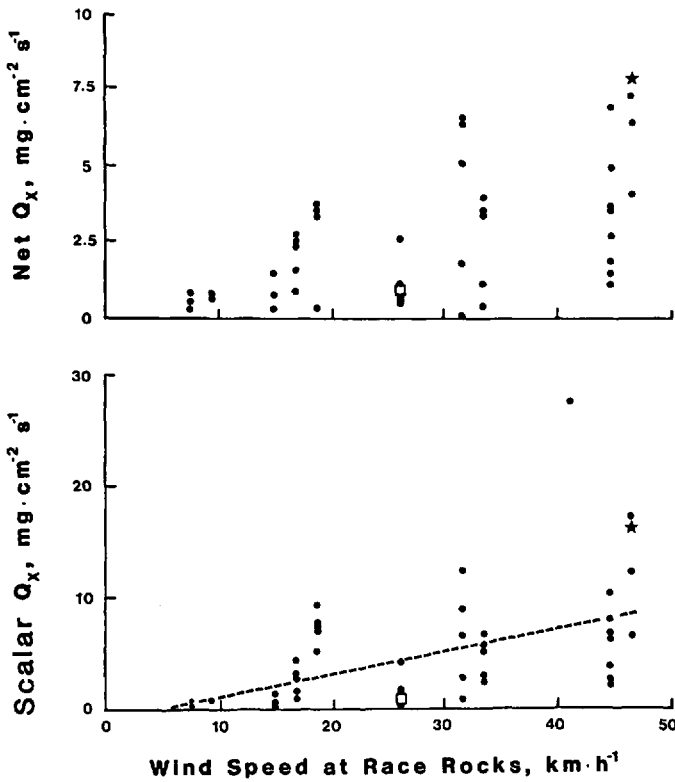


Figure 6. Net and scalar sediment fluxes at False Bay as a function of wind speed at Rack Rocks Lightstation. Special symbols are the same as in Figure 5. Dashed line (lower panel) indicates the empirical fit (Eq. 3) to the scalar flux data.

preferable (Sleath, 1984). Based on linear theory then, from a height of 15 cm above the bottom to just outside the wave boundary layer, the oscillatory velocity field is uniform to within 1%. Thus the flow measurements of the electromagnetic current meter accurately reflect flow in much of the region of interest (i.e., within 3.5 cm of the bottom). The height of the wave boundary layer was calculated to be  $\delta_w = \kappa u_* / \omega$ , where  $\kappa$  is von Karman's constant (0.4),  $u_*$  is the shear velocity, and  $\omega$  is the wave frequency ( $2\pi/T$ ). An estimate of shear velocity is needed (it is clearly greater than the critical shear velocity for the sediments,  $1.17 \text{ cm s}^{-1}$ , Miller, 1985) and can be calculated from measured flows using friction coefficients. Alternatively, we observed the dominant bed roughness to be due to vortex sediment ripples, approximately 1.5 cm high and 8 cm in wavelength. Using an analogy from steady hydraulically rough flow,  $z_0$  should be approximately one-thirtieth of the ripple height, here  $z_0 = 0.05 \text{ cm}$ . If we assume the velocity in the wave boundary layer to be logarithmic (Grant and Madsen, 1979, 1982;

and ignoring movable bed roughness, etc.), the velocity at  $\delta_w$  must match that of the outer, oscillatory flow. This constraint determines the value of  $u_*$ , which for the maximum (near-bottom) oscillatory velocity for the specified wave ( $20.9 \text{ cm s}^{-1}$ ) yields  $u_* = 3.36 \text{ cm s}^{-1}$ , about three times the critical value for the sediments. Accordingly, the estimated thickness of the wave boundary layer  $\delta_w$  is 0.60 cm. Thus the velocity field within 3.5 cm of the bottom is: 99% of that measured at 15 cm to  $\delta_w = 0.6 \text{ cm}$  above the bottom, and  $u = (u_*/\kappa) \ln(z/z_0)$  below  $\delta_w$ .

The suspended sediment concentration profile below 3.5 cm was not measured, but using established suspended sediment concentration models, can be extrapolated from our measurements. Use of these models is reasonable in light of the calculated Rouse parameter (Muschenheim, 1987)  $w_s/\kappa u_* = 0.8$  ( $w_s$  is the settling velocity,  $1.07 \text{ cm s}^{-1}$ , Miller, 1985 from equations of Gibbs *et al.*, 1971), values less than one generally indicating suspended load transport (in steady flows). Two models, concentration as an exponential function of height and concentration as a power function of height (Sleath, 1984), were fit to the mean concentration profiles for the full 9.4 min run data set. The accuracy of the fits was high ( $r^2 = 0.998$  and  $0.949$ , respectively, five observations each), but these equations predict quite different concentration values near the bed; note that the power function has a singularity at the bed. Specifically, the equations determined were:  $C(z) = 2.082 \cdot \exp(-0.108 z)$  and  $C(z) = 4.067 \cdot z^{-0.799}$ ; units are  $\text{mg cm}^{-3}$ .

We calculated fluxes from the velocity and the two concentration profiles specified above. These horizontal, instantaneous fluxes were numerically integrated from  $z_0$  to the height of the lowest suspended sediment sensor (3.5 cm) and compared with a simple estimate of the product of the velocity at 15 cm and the concentration at 3.5 cm (times 3.5 cm to vertically integrate, as was done with our computations with field data). As expected, the approximate estimate underestimates the theoretical, calculated flux, by 9% for the exponential concentration profile and by 56% for the power function profile. We varied the height of the wave entered in the calculations, using the average wave height, the significant wave height, and the average height of the one-tenth highest waves ( $a = 4.0, 6.4, \text{ and } 8.15 \text{ cm}$ ). We also varied the value of shear velocity imposed on the wave boundary layer (here calculating  $z_0$  such that the velocity profiles match at the top of the wave boundary layer) from twice to four times the critical shear velocity. Over all these calculations, the maximum errors (underestimate) were 13% (exponential concentration profile) and 63% (power function profile). Because we extrapolated below the height at which concentrations were measured, the predicted concentrations are quite sensitive to the coefficients of the model curves. Plots of the logarithm of mean concentrations with height (this corresponds to the exponential model above) from sedimentologically active runs indicated that although the concentration levels varied between runs, the profiles were remarkably parallel. In other words, the exponential coefficient varied little between runs, and hence calculations based on the profile used should yield reasonable error estimates.

It is more difficult to assess the accuracy of the vertical flux estimates. If concentration profiles are essentially uniform below 3.5 cm during a suspension event, then there is little error in the resulting estimates. If the instantaneous concentration increases toward the bed during suspension, then we underestimate the vertical flux, the degree of which depends on the magnitude of the concentration gradient. It seems presumptive to use a mean concentration profile to approximate the instantaneous concentration profile during active suspension events. This analysis assumes lateral homogeneity in the suspension event, i.e., no horizontal gradients in suspended sediment concentration. This is reasonable since the near bottom orbital amplitude for the specified condition is approximately equal to the ripple wavelength (i.e., plumes of sediment suspended from a ripple crest reach the adjacent crest, Sleath, 1984) and hence the sensor averages over concentrations over two sediment ripples. Further, we have observed resuspension events in quite shallow water (less than 20 cm) in which initially distinct plumes of suspended sediment are effectively mixed in an interval of time shorter than a wave period (2–3 s).

Thus the instantaneous, horizontal flux (at the velocity maximum) appear accurate to within a factor of three, and mean values computed from these instantaneous fluxes should likewise be that accurate. Given the uncertainties in the above calculations, it does not seem appropriate to apply any sort of adjustment to the raw flux estimates, neither horizontal nor vertical. Assumptions made to extrapolate suspended sediment concentrations below the lowest sensor are even more tenuous for the estimation of bias in rapidly varying vertical flux estimates. A profitable approach may be a more detailed analysis and modelling of the suspended sediment time series data, an effort which goes far beyond the scope of this paper. In the following discussion all flux estimates are employed in relative comparison or as order of magnitude estimates. However, none of the qualitative conclusions we draw from the data would change if above indicated adjustments were made to the empirical estimates.

To compare our horizontal sediment flux estimates with literature values, we note that wave-induced oscillatory flows correlate well with sediment movement (Fig. 4) and fluxes (Fig. 5 and Table 1) and can be used to predict these flux rates. In previous studies, the average (volumetric) transport rate over a wave half cycle  $Q$  has been modeled as:

$$Q/w_s d = c\Psi^3, \Psi > \Psi_{cr} \quad (1)$$

where transport rate has been scaled by particle settling velocity  $w_s$  and grain diameter  $d$ ; and  $\Psi$  is the Shields parameter (nondimensional bottom shear stress,  $\Psi = \tau/[(\rho_s - \rho)gd]$ , where  $\tau$  is the boundary shear stress and  $\rho_s$  is the sediment grain density (Madsen and Grant, 1977). The coefficient  $c$  is a constant when  $\Psi$  is greater than twice the critical value  $\Psi_{cr}$ . In an effort to see if our measured transport rates scale with flow velocity in a manner similar to that in published relationships, we took the mean bottom stress as proportional to the velocity variance,  $U_w^2$  (i.e., assuming a



constant friction factor, Jonsson, 1966), converted our scalar flux rates to a volumetric basis (by dividing by the sediment bulk density,  $1.6 \text{ g cm}^{-3}$  from Miller, 1985) and vertically integrated them (by multiplication by the height of the lowest sensor, 3.5 cm) to obtain a "bedload" transport rate. We then fitted this converted False Bay scalar flux data (i.e.,  $Q = Q_x \times 3.5 \text{ cm}/1.6 \text{ g cm}^{-3}$ ) to the form of Eq. (1) and found the best fit to be:

$$Q/w_s d = 9.45 \times 10^{-2} (s_u^2/[\rho_s - \rho]gd)^{1.57}, r^2 = 0.90 \quad (2)$$

for a settling velocity of  $1.07 \text{ cm s}^{-1}$ , median grain size of  $143 \text{ }\mu\text{m}$ , grain density of  $2.65 \text{ g cm}^{-3}$ , and a fluid density of  $1.02 \text{ g cm}^{-3}$ . A critical value was not included in Eq. (2) because the fitted variables are mean quantities. Since a distribution of wave heights and the associated near-bottom velocities is characterized by the measured velocity variance, no single value of the variance can be a threshold condition. The value of the exponent (approximately a  $u^{2 \times 1.57}$ , for Eq. (2) or  $u^{3.2}$  dependence) is quite reasonable inasmuch as observed transport rates are intermediate between those modeled by Madsen and Grant (1977, a  $u^6$  dependence) and Vincent *et al.* (1981,  $u^3$ ). Thus it is apparent that our flux estimates scale with wave velocities in a manner consistent with previous results, though it is difficult to compare directly equation coefficients or rate estimates from various empirical equations.

*d. Extrapolation to annual patterns of sediment transport.* Before we can generalize from the October 1984 results, it is important to determine if they are representative of other times in the year. To do this, we used an empirical, linear relationship between wind speed at Race Rocks and sediment flux at False Bay. This relationship is illustrated in Figure 6 (lower panel) and was determined to be:

$$Q_x [\text{mg cm}^{-2} \text{ s}^{-1}] = 0.214 \cdot (W - 6.3), \quad W > 6.3 \text{ km h}^{-1}, r^2 = 0.26. \quad (3)$$

We focus on the wave-generated scalar flux since it is well explained in terms of existing sediment transport models (Eq. 2) and because we lacked the spatial array of field instruments needed to understand the mean circulation within the bay and its contribution to the net sediment flux. Also, detailed modeling of the relationship between transport rates and wind, wave, and tide conditions appears unnecessarily complex for the present purposes. Admittedly, a large fraction of the variance (in excess of 70%) in transport rate is unexplained by wind speed: this is graphically apparent in the scatter in Figure 6. This low predictive value is due largely to the poor relationship between wind speed and wave conditions, not the relationship between wave conditions and sediment flux (Table 1). Since we obtained data only from a limited period of time (which fortunately included a variety of wind conditions), using Eq. 3 and monthly climatological records of wind speed seems to be the best available way to extrapolate our October results to other times of the year. Such extrapolations would clearly change if other equations were fit to these data or, better yet, if

additional data were available. We believe however that regardless of the threshold or slope values used extrapolated results would represent valid comparisons between months.

Using climatological data in the form of monthly percentage occurrence in a speed class at Race Rocks (1982–1978), we calculated the percentage of time winds exceeded the above threshold (using the nearest tabulated class break at  $6 \text{ km h}^{-1}$ ). This percentage peaked in July and January (95%) between minima in March (89%) and October (84%). Mean monthly transport rates calculated from weather records revealed a similar seasonal pattern, with year-to-year variability about one-third of that among months. Sediment transport rates like those observed at False Bay in October 1984 are thus apparently not exceptional. The sediment transport rate monthly averages range from a high of  $4.7 \text{ mg cm}^{-2} \text{ s}^{-1}$  in July to a low of  $2.2 \text{ mg cm}^{-2} \text{ s}^{-1}$  in September. The mean for all runs (over only four days) for October 1984 is  $4.7 \text{ mg cm}^{-2} \text{ s}^{-1}$  (cf. October's five-year average of  $2.2 \text{ mg cm}^{-2} \text{ s}^{-1}$ ). High winds are associated with the passage of winter storm systems through the region (as they did in the 4-day field sampling period) and cause significant transport. In the summer, high winds are associated with westerly afternoon and evening sea breeze (Thomson, 1981; Price and Hylleberg, 1982; Lilly, 1983). According to our data, these winds should be of sufficient strength and duration to generate waves in the strait large enough to cause sediment transport in False Bay. These calculations need to be verified for periods outside the time of year on which the empirical Eq. (3) was based before they can be considered to be completely reliable; we employ them here for comparative purposes in the spirit of rough approximation (Harte, 1985). Our method of calculation results in averages over the time that water covers the field site. Since the site is very nearly at mean water level, multiplication of these values by 0.5 converts them to averages over the entire tidal cycle.

One factor which is likely to vary from season to season is the extent of microbial binding due to benthic diatoms and bacteria and their effect on the critical erosion velocity of the sediments (W.D. Grant *et al.*, 1982; J. Grant *et al.*, 1986). Our measurements coincided both with the passage of storms and with the annual autumn change from daytime to nighttime low tides in Puget Sound. Algal adhesion was much in evidence (as a brownish coloration of surficial sediments) during the first day of the study. By the end of the study, no algal film could be seen. This observation concurs with that of Grant *et al.* (1986) and may account for some of the scatter in Figures 5 and 6.

*e. Ecologically-relevant sediment fluxes and biological implications.* To make a gross comparison of geophysical and biological sediment processing rates, we use the flux data from our experiment and the published feeding rate data from animals collected at False Bay. Deposit feeding at the instrument site in False Bay was dominated by two species: *Pseudopolydora kempji japonica* and *Abarenicola pacifica*.

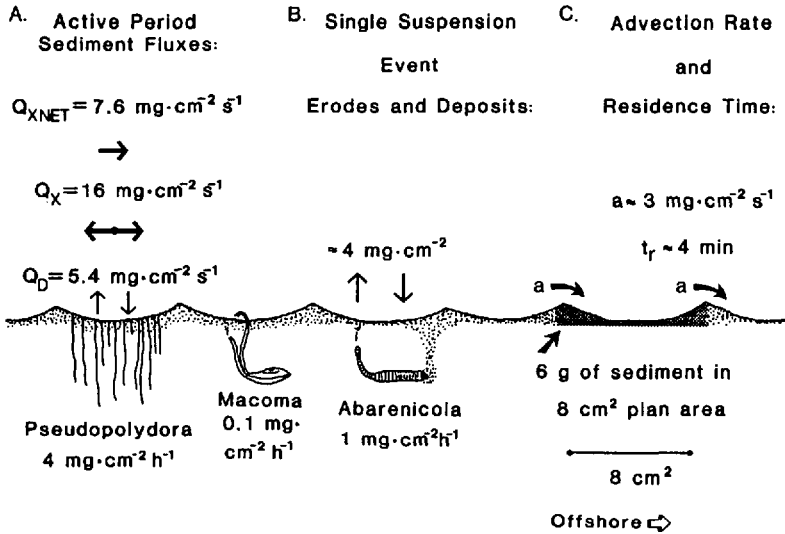


Figure 7. Geophysical sediment fluxes (top) and estimated biological sediment processing rates (bottom) calculated (see text for details) for data collected 1240 PDT 28 October 1984. (A) Fluxes averaged over the 9.4-min data collection period. (B) Amount of material suspended and deposited in one suspension event. (C) Illustration of the advection rate and residence time of a sediment particle in the pool of particles available to an individual *Pseudopolydora* under such sediment transport conditions. For comparison with other sediment transport observations, these data are from that run depicted in Figure 4 and indicated by stars in Figures 5 and 6. Sediment transport rates here (relative to feeding rates) are such that any surface manifestation of feeding (fecal pellets, mounds, or feeding funnels) is immediately erased, and hence no effect of feeding on the sediment surface is illustrated.

The feeding biology of both the species at False Bay has been well studied (e.g., Taghon *et al.*, 1980; Taghon, 1982; Taghon and Jumars, 1984; Jumars and Self, 1986; Miller and Jumars, 1986; and Hobson, 1967). Published results may be used to estimate feeding rates: in laboratory experiments at 10–12°C, *Pseudopolydora* fed at a maximum rate of  $4 \text{ mg h}^{-1} \text{ worm}^{-1}$ ; field abundances are typically  $1 \text{ worm cm}^{-2}$  (Miller and Jumars, 1986). On an areal basis then, *Pseudopolydora* consume at most  $4 \text{ mg cm}^{-2} \text{ h}^{-1}$ . We note that this hourly rate is of the same numerical magnitude as the measured field flux rates *per second* during active transport (cf. Fig. 5). In other words, and as illustrated diagrammatically in Figure 7a, during periods of active sediment transport at False Bay, more sediment passes by (in horizontal transport in a  $1 \text{ cm}^2$  area), or is deposited on the bed and resuspended over a worm in a single second than that worm would feed upon in an entire hour.

In a single suspension event (as illustrated in Fig. 7b), sediment concentration can rise from zero to  $10 \text{ g l}^{-1}$  at 3.5 cm above the bed in a fraction of a second. This change in sediment concentration requires the erosion of *at least* 35 mg of sediment (over a unit cross-stream width of say, 1 cm) from the bottom, most likely from ripple crests. If

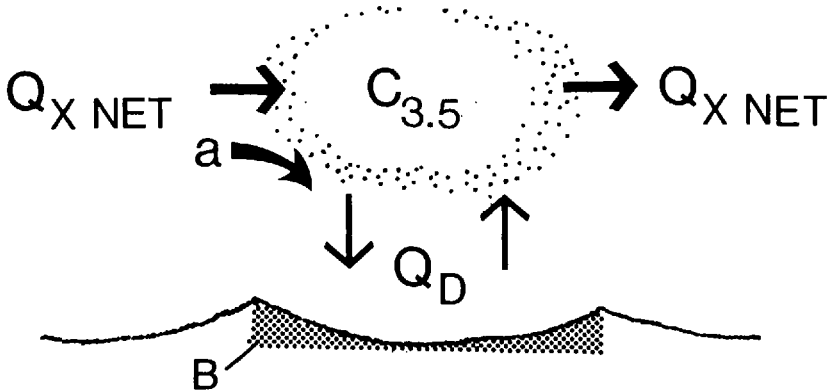


Figure 8. Calculation of flux rate of new sediment and food resources to an individual deposit feeder. From this schematic diagram, one can see that the flux of sediment into the "cloud" of suspended sediment above the bed (denoted  $C_{3.5}$ ) is  $Q_{XNET} + Q_D$ . Likewise, the flux to the bed (B) from the cloud is  $Q_D$ . If the cloud is well-mixed, then the fraction of the sediment in the cloud that is advected from upstream—that is, contributed by  $Q_{XNET}$ —is  $Q_{XNET}/(Q_{XNET} + Q_D)$ . Thus the flux of newly advected sediment to the bed,  $a$ , is  $Q_D$  times the fraction of  $C_{3.5}$  that is advected:  $a = (Q_{XNET}/[Q_{XNET} + Q_D]) \cdot Q_D$ . See text for a numerical calculation and the discussion of the implications of this result. This box model was used to calculate advection rates and residence time illustrated in Figure 7C.

this material is deposited uniformly over the rest of the ripple (say, 8 cm in length by 1 cm wide), the amount of material deposited ( $4 \text{ mg cm}^{-2} \text{ event}^{-1}$ ) is still as much as that amount of sediment consumed by the worms in an hour. Therefore, sediment transport rates exceed feeding rates by a factor of  $10^3$ – $10^4$ . Similar calculations may be made for *A. pacifica* as well as for *Macoma nasuta*, a surface-deposit feeding tellinid bivalve also present at the field site (see Fig. 7; for feeding rate data, see Hobson, 1967 and Hylleberg and Gallucci, 1975, respectively).

A similar, but more precise calculation of ecologically important flux rates can be made using a box model with two compartments (Fig. 8). Under transport conditions like those in Figure 4 (summarized in Fig. 7a), sediment is suspended periodically and well mixed by turbulence. In an average sense though, there is a cloud of suspended sediments above the bed (one box of the compartmental model), the concentration (denoted  $C_{3.5}$ ) of which is measured by the lowest suspended sediment sensor. This cloud of sediment vertically exchanges particles with the bed (the other box of the model) via deposition and erosion. The net horizontal flux of sediment into the resuspended cloud of sediment above the bed is  $Q_{XNET}$ , and the rate of deposition and erosion at the bed is  $Q_D$ . The amount of sediment that is advected from upstream and deposited on the bed (and not merely resuspended and redeposited) is the ecologically-relevant advection rate of sediments (Miller *et al.*, 1984). If the total (not net) deposition rate ( $Q_D$ ) is zero, then no sediment from upstream is deposited on the bed, regardless of the net transport rate (i.e., there is no exchange with the bed). If however,

deposition and net transport rates are equal, then on average half of the sediment advecting from upstream will be deposited on the bed. Thus the fraction of all suspended sediment that is newly advected sediment is the ratio of the net flux ( $Q_{XNET}$ ) to the sum of all flux rates ( $Q_{XNET} + Q_D$ ). Accordingly, the net rate of newly advected material depositing on the bed is that fraction times the deposition rate ( $Q_D$ ). For example (Fig. 7c), using flux rates for the run illustrated in Figure 4,  $Q_{XNET} = 7.6 \text{ mg cm}^{-2} \text{ s}^{-1}$  and  $Q_D = 5.4 \text{ mg cm}^{-2} \text{ s}^{-1}$ , the fraction of newly advected suspended sediment is 0.59 and calculated advection rate  $a$  is  $3.2 \text{ mg cm}^{-2} \text{ s}^{-1}$ . For a typical *Pseudopolydora* feeding area of  $6.2 \text{ cm}^2$  (Miller and Jumars, 1986) and an individual feeding rate of  $4 \text{ mg worm}^{-1} \text{ h}^{-1}$ , the estimated ratio of advection to ingestion is  $1.8 \times 10^4$ . Clearly, advection rate greatly exceeds ingestion rate. While not included in the preceding calculations, we expect the effect of selective feeding to be of second-order. Though demonstrating a preference for smaller particles (e.g., Taghon, 1982), spionids readily consume particles even much larger than the median grain size of sediments at the field site.

The mean time a particle is accessible to a given deposit feeder, its residence time (as defined by Miller *et al.*, 1984) can be estimated from the above advection rate and appropriate individual-worm particle pool size. As a generous estimate of the amount of sediment in the active pool we take that of a whole cat's back ripple, 8 cm long, 1 cm wide and 1 cm high (see Fig. 7). Assuming a shallow V-shaped triangular cross-section and a bulk density of  $1.6 \text{ g cm}^{-3}$ , this ripple contains  $4 \text{ cm}^3$  or 6.3 g of sediment over a plan area of  $8 \text{ cm}^2$ . When advection is much greater than ingestion, residence time  $t_r = N/a$ , where  $N$  is the particle pool size (here, the active resuspension layer, or  $6.3 \text{ g}/8 \text{ cm}^2 = 0.79 \text{ g cm}^{-2}$ ), is  $0.79 \text{ g cm}^{-2}/3.2 \text{ mg cm}^{-2} \text{ s}^{-1} = 247 \text{ s}$  or about 4 minutes. This is much shorter than the microbial doubling time against which it is scaled by Miller *et al.* (1984) to predict the relative importance of advected and locally-produced food sources. If the pool is smaller, then the residence time will be proportionately shorter. Selection for smaller particles should decrease both the effective pool size and advection rate so its effect on residence time may be difficult to predict. This calculation is in rough agreement with the observed movement of tracer particles matched in critical shear stress and settling velocity to that of False Bay sediments (Miller, in prep.). Even under very modest wave conditions, a significant fraction (4–27%) of these particles dispersed 20 cm or more from their release point within 30 minutes. Net flow during this experiment caused more particles to move offshore than on.

In summary, this analysis suggests that there are many periods when sediment transport due to waves grossly exceeds the maximal rate of deposit feeding. As Miller and Jumars (1986) demonstrate, deposit-feeding rate may be depressed by fecal accumulation whenever two or more hours pass without appreciable flow or sediment transport. An exact calculation of the percentage of time during the year when conditions exist is not possible from the limited data at hand. Based on the results

obtained in this study and the additional, relatively low levels of sediment transport that occur with tidal immersion and emersion (e.g., Anderson, 1980; Anderson and Mayer, 1984; Wissmar and Simenstad, 1985), we conclude that only rarely is feeding rate limited by sediment supply or fecal removal while water covers the site. The fluid and sedimentological measurements available, when coupled with laboratory observations (Miller and Jumars, 1986) suggest that competition for food by surface deposit feeders will be moderated by waves. Food limitation will be rare under conditions of active transport. If it occurs at all, it will be during especially quiescent periods or in tidal pools or the exposed sandflat surface.

The reported flux rates and tracer particle observations suggest that sediment particles from some distance away may be transported and deposited in an individual's feeding area and serve as a food source. The upstream (or surrounding) benthic community, particularly the microflora and deposit feeders, may differ, as may the food resources transported from there. A more sophisticated analysis of the spatial variation in deposit feeder abundance and feeding rate, microbial growth rates, and sediment transport (both advective and dispersive) will be needed to identify the lateral extent to which deposit feeders share food resources. Methods exist which can measure the relevant biological rates, but probably the most serious limitation at present to such an analysis is in the parameterization, measurement, and modelling of the appropriate geophysical processes.

In addition to its implications for feeding biology, the persistence of fecal mounds on the sediment surface has been implicated in structuring the infaunal community around *A. pacifica* burrows (Brenchley, 1981; Wilson, 1981; but see Woodin, 1985). Material defecated at a rate of  $142 \text{ mg h}^{-1}$  (Hobson, 1967) over  $1 \text{ cm}^2$  would be easily dispersed by the measured sediment transport rates. Individual fecal mounds, even large ones produced during low tide, are unlikely to exist during active sediment transport periods at False Bay. Further, the fact of ripple migration suggests that animals will be well adapted to occasional burial by depths of sediments comparable to those seen in mounds, downplaying the importance of biogenic mounds in structuring communities experiencing frequent, physical sediment transport.

*f. Implications for further research.* There are many desirable refinements to the rough calculations of the preceding section. Annual (e.g., reproductive, ontogenetic, and temperature-dependent) components of the functional and numerical responses of deposit feeders need to be measured in the field. Sediment transport measurements should be extended to more portions of the year and nearer to the bed, and they should be made on a scale more closely approximating an animal's feeding area. The potential importance of sediment transport suggested by Grant (1983) and our preliminary measurements and calculations indicate that the effort to make these refinements would be worthwhile. Grant (1985) describes a new technique which he has used successfully to measure the geophysical incorporation of organic matter into marine

sediments. Comparison of our measurements of sediment transport with other studies must be made carefully. The measures of gross and net transport are highly technique-dependent. Knowledge of the time period (and even interval) over which averages are made is critically important. Transport phenomena are highly variable in time (and space) and inherently nonlinear. Most studies and our summary calculations report only the magnitude of sediment transport. They omit important variables, at least to the biology of benthic organisms, such as the interval between sediment transport events.

With regard to benthic organisms, we first consider those which feed at the sediment surface. A review of what is known about the response of *P. kempji japonica* and of other deposit feeders to fluid and particulate fluxes, in the light of the present measurements, reveals a surprising lack of observations on organism feeding behavior in wave-dominated environments. While there is information on organism behavior under steady, unidirectional flow (Taghon *et al.*, 1980; Dauer *et al.*, 1981; Dauer, 1983, 1985), there are no observations of organism behavior in oscillatory (wave) boundary layers (*sensu* Nowell and Jumars, 1984). The elegant arguments of Grant and Madsen (1979, 1982) show that knowledge of particle transport in steady flows can readily be used to predict particle motion under oscillatory flow (due to the essentially instantaneous response of particle motion to fluid motion). It is unlikely, however, that one can similarly extrapolate from observed behaviors in steady flows to those in wave-dominated environments. It is not known, for example, whether the helically coiled palp posture used by *P. kempji japonica* to suspension feed under steady, particle-laden flows (Taghon *et al.*, 1980) is used when current direction oscillates with the wave period. Even qualitative observations would be helpful at this point. There are no studies of feeding behavior of any surface-deposit feeder in oscillatory flow.

Secondly, deposit feeders which consume sediment below the sediment-water interface should be less tightly coupled to geophysical transport phenomena. In general, a longer lag time can be expected between events at the surface and feeding responses. In a funnel-feeding mode, however, *Abarenicola pacifica* feeds on material that was recently deposited on the surface and therefore may be influenced relatively rapidly by sediment transport. These sorts of responses have not received observational attention, largely because of logistical difficulties (Jumars and Self, 1986). Also, the straightforward approach of quantifying feeding rate from egestion rate is not feasible when egested material is transported away or rapidly dispersed.

Suspension-feeding organisms and their food resources are directly and intimately linked to mixing and resuspension processes near the bottom. This interaction has been a long-standing interest among benthic ecologists (e.g., Rhoads and Young, 1970; Wildish and Kristmanson 1979, 1984) and has experienced a recent resurgence in both field (e.g., Peterson and Black, 1987) and laboratory (e.g., Muschenheim, 1987; Fréchet *et al.*, 1988) study. As in deposit-feeding studies, recent work has concen-

trated on steady, unidirectional flow conditions. The striking differences in the rates of turbulent mixing and boundary layer thickness found in oscillatory flow should be ample justification for studying shallow-water suspension feeders in this alternative flow regime.

Lastly, sediment transport has been implicated in the abrasion of microbes from exposed grain surfaces (e.g., Munro *et al.*, 1978; Miller, in prep.). Most of these past observations come from environments with high rates and frequencies of transport, such as wave-exposed coasts. The degree to which storms and associated sediment transport events affect epipsammic microbial abundances, and consequent food abundance and quality for deposit feeders, in False Bay and in most other marine environments is not yet known.

#### 4. Conclusions

The benthic environment in False Bay is dominated by oscillatory flows and, during periods of high winds, relatively large waves and active sediment transport. Flow and sediment transport conditions respond quickly and dramatically to the local weather. Seasonally, winter and summer are the periods of highest winds, though there is much year-to-year variability superimposed on the annual cycle. During storms, sediment fluxes exceed biological processing rates of sediment by a factor of  $10^3$ – $10^4$ . The average time for which a given particle is available to a deposit feeder may be only a few minutes. The benthic environment in False Bay ranges from one dominated by wind-wave transport of sediments to one in which rates of biological and geophysical transport of sediments are closely matched. We expect that feeding rate of *P. kempfi japonica* will be limited rarely by particle supply or by fecal accumulation. The extent of physical sediment transport, wave-driven in many benthic environments, provides the backdrop against which biogenic sediment modifications should be viewed. In False Bay this perspective suggests that neither local biogenic burial events nor competition for food among deposit feeders will be strong forces structuring the benthic community.

*Acknowledgments.* We thank R. Beach, R. Johnson, P. Jumars, M. Miller, D. Penry and L. Self for invaluable assistance at False Bay. P. Jumars, A. Nowell and D. Strathmann contributed comments which materially improved this manuscript. B. Burton provided access to weather data. We also thank the director and staff of Friday Harbor Laboratories, University of Washington, for use of their facilities as a home base. This research was supported by NSF Grant OCE-86-08157 to P. Jumars and A. Nowell and is contribution 1782 from the School of Oceanography, University of Washington.

#### REFERENCES

- Anderson, F. E. 1980. The variation in suspended sediment and water properties in the flood-water front traversing the tidal flat. *Estuaries*, 3, 28–37.



- Anderson, F. E. and L. M. Mayer. 1984. Seasonal and spatial variability of particulate matter of a muddy intertidal flood front. *Sedimentology*, *31*, 383–394.
- Beach, R. A. and R. W. Sternberg. 1988. Suspended sediment transport in the surf zone: response to cross-shore infragravity motion. *Mar. Geol.*, *80*, 61–79.
- Brenchley, G. A. 1981. Disturbance and community structure: An experimental study of bioturbation in marine soft-bottom environments. *J. Mar. Res.*, *39*, 767–790.
- Dauer, D. M. 1983. Functional morphology and feeding behavior of *Scolecopsis squamata* (Polychaeta: Spionidae). *Mar. Biol.*, *77*, 279–285.
- 1985. Functional morphology and feeding behavior of *Paraprionospio pinnata* (Polychaeta: Spionidae). *Mar. Biol.*, *85*, 143–151.
- Dauer, D. M., C. A. Maybury and R. M. Ewing. 1981. Feeding behavior and general ecology of several spionid polychaetes from the Chesapeake Bay. *J. Exp. Mar. Biol. Ecol.*, *54*, 21–38.
- Dean, R. G. and R. A. Dalrymple. 1984. *Water Wave Mechanics for Engineers and Scientists*. Prentice-Hall., 353 pp.
- Downing, J. P., Jr. 1983. Field studies of suspended sand transport, Twin Harbors Beach, Washington. Ph.D. dissertation, Univ. Washington, Seattle. 122 pp.
- Downing, J. P., Jr., R. W. Sternberg and C. R. B. Lister. 1981. New instrumentation for the investigation of sediment suspension processes in the shallow marine environment. *Mar. Geol.*, *42*, 19–34.
- Fréchette, M., C. A. Butman and W. R. Geyer. 1988. The importance of boundary-layer flow processes in supplying phytoplankton to the benthic suspension-feeder, *Mytilus edulis*. *Limnol. Oceanogr.*, (in press).
- Gibbs, R. J., M. D. Mathews and D. A. Link. 1971. The relationship between sphere size and settling velocity. *J. Sed. Pet.*, *41*, 7–18.
- Grant, J. 1983. The relative magnitude of biological and physical sediment reworking in an intertidal community. *J. Mar. Res.*, *41*, 673–689.
- 1985. A method for measuring horizontal transport of organic carbon over sediments. *Can. J. Fish. Aquat. Sci.*, *42*, 595–602.
- Grant, J., U. V. Bathmann and E. L. Mills. 1986. The interaction between benthic diatom films and sediment transport. *Est. Coastal Shelf Sci.*, *23*, 225–238.
- Grant, W. D., L. F. Boyer and L. P. Sanford. 1982. The effects of bioturbation on the initiation of motion of intertidal sands. *J. Mar. Res.*, *40*, 659–677.
- Grant, W. D. and O. S. Madsen. 1979. Combined wave and current interaction with a rough bottom. *J. Geophys. Res.*, *84*, 1797–1808.
- 1982. Movable bed roughness in unsteady oscillatory flow. *J. Geophys. Res.*, *87*, 469–481.
- Hanes, D. M. and D. A. Huntley. 1986. Continuous measurements of suspended sand concentration in a wave dominated nearshore environment. *Cont. Shelf Res.*, *6*, 585–596.
- Harte, J. 1985. *Consider a Spherical Cow*. William Kaufmann, Inc. 283 pp.
- Hobson, K. D. 1967. The feeding and ecology of two North Pacific *Abarenicola* species (Arenicolidae, Polychaeta). *Biol. Bull.*, *133*, 343–354.
- Hylleberg, J. 1975. Selective feeding by *Abarenicola pacifica* with notes on *Abarenicola vagabunda* and a concept of gardening in lugworms. *Ophelia*, *14*, 113–137.
- Hylleberg, J. and V. F. Gallucci. 1975. Selectivity in feeding by the deposit-feeding bivalve *Macoma nasuta*. *Mar. Biol.*, *32*, 167–178.
- Jonsson, I. G. 1966. Wave boundary layers and friction factors. *Proc. Coastal Eng. Conf. 10th*, *1*, 127–148.
- Jumars, P. A. and R. F. L. Self. 1986. Gut-marker and gut-fullness methods for estimating field

- and laboratory effects of sediment transport on ingestion rates of deposit feeders. *J. Exp. Mar. Biol. Ecol.*, *98*, 293–310.
- Jumars, P. A., R. F. L. Self and A. R. M. Nowell. 1982. Mechanics of particle selection by tentaculate deposit feeders. *J. Exp. Mar. Biol. Ecol.*, *64*, 47–70.
- Lilly, K. E., Jr. 1983. *Marine Weather of Western Washington*. Starpath. 150 pp.
- Madsen, O. S. and W. D. Grant. 1977. Quantitative description of sediment transport by waves. *Proc. Coastal Eng. Conf. 15th.*, *2*, 1093–1112.
- Miller, D. C. 1984. Mechanical post-capture particle selection by suspension- and deposit-feeding *Corophium*. *J. Exp. Mar. Biol. Ecol.*, *82*, 59–76.
- 1985. Interactions of marine sediment transport with deposit feeding and microbial growth. Ph.D. dissertation, Univ. Washington, Seattle. 156 pp.
- Miller, D. C. and P. A. Jumars. 1986. Pellet accumulation, sediment supply and crowding as determinants of surface deposit-feeding rate in *Pseudopolydora kempji japonica* Imajima & Hartman (Polychaeta, Spionidae). *J. Exp. Mar. Biol. Ecol.*, *99*, 1–17.
- Miller, D. C., P. A. Jumars and A. R. M. Nowell. 1984. Effects of sediment transport on deposit feeding: scaling arguments. *Limnol. Oceanogr.*, *29*, 1202–1217.
- Munro, A. L. S., J. B. J. Wells and A. D. McIntyre. 1978. Energy flow in the flora and meiofauna of sandy beaches. *Proc. R. Soc. Edinburgh*, *76B*, 297–315.
- Muschenheim, D. K. 1987. The dynamics of near-bed seston flux and suspension-feeding benthos. *J. Mar. Res.*, *45*, 473–496.
- National Oceanic and Atmospheric Administration. 1983. *Tide Tables 1984. West Coast of North America and South America*. U. S. Dept. Commerce. 232 pp.
- Nowell, A. R. M. and P. A. Jumars. 1984. Flow environments of aquatic benthos. *Ann. Rev. Ecol. Syst.*, *15*, 303–328.
- Pamatmat, M. M. 1966. The ecology and metabolism of a benthic community on an intertidal sandflat (False Bay, San Juan Island, Washington). Ph.D. dissertation, Univ. Washington, Seattle. 244 pp.
- 1968. Ecology and metabolism of a benthic community on an intertidal sand flat. *Int. Rev. Ges. Hydrobiol.*, *53*, 211–298.
- Parker, B. B. 1977. *Tidal hydrodynamics in the Strait of Juan de Fuca-Strait of Georgia*. NOAA Technical Rep. NOS-69.
- Peterson, C. H. and R. Black. 1987. Resource depletion by active suspension feeders on tidal flats: influence of local density and tidal elevation. *Limnol. Oceanogr.*, *32*, 143–166.
- Price, L. H. and J. Hylleberg. 1982. Algal-faunal interactions in a mat of *Ulva fenestrata* in False Bay, Washington. *Ophelia*, *21*, 75–88.
- Rhoads, D. C. and D. K. Young. 1970. The influence of deposit-feeding organisms on sediment stability and community trophic structure. *J. Mar. Res.*, *28*, 150–178.
- Sleath, J. F. A. 1984. *Sea bed Mechanics*. John Wiley & Sons. 335 pp.
- Taghon, G. L. 1982. Optimal foraging by deposit-feeding invertebrates: roles of particle size and organic coating. *Oecologia*, *52*, 295–304.
- Taghon, G. L. and P. A. Jumars. 1984. Variable ingestion rate and its role in optimal foraging behavior of marine deposit feeders. *Ecology*, *65*, 549–558.
- Taghon, G. L., A. R. M. Nowell and P. A. Jumars. 1980. Induction of suspension feeding in spionid polychaetes by high particulate fluxes. *Science*, *210*, 262–264.
- 1984. Transport and breakdown of fecal pellets: biological and sedimentological consequences. *Limnol. Oceanogr.*, *23*, 752–759.
- Thomson, R. E. 1981. *Oceanography of the British Columbia Coast*. Can. Spec. Publ. Fish. Aquat. Sci., *56*, 291 pp.

- Vincent, C. E., R. A. Young and D. J. P. Swift. 1981. Bedload transport under waves and currents. *Mar. Geol.*, *39*, M71–M80.
- Wildish, D. J. and D. D. Kirstmanson. 1979. Tidal energy and sublittoral macrobenthic animals in estuaries. *J. Fish. Res. Bd. Can.*, *36*, 1197–1206.
- 1984. Importance to mussels of the benthic boundary layers. *Can. J. Fish. Aquat. Sci.*, *41*, 1618–1625.
- Wilson, W. H., Jr. 1981. Sediment-mediated interactions in a densely populated infaunal assemblage: the effects of the polychaete *Abarenicola pacifica*. *J. Mar. Res.*, *39*, 735–748.
- 1982. The role of density dependence in a marine infaunal community. *Ecology*, *64*, 295–306.
- 1984. Non-overlapping distributions of spionid polychaetes: the relative importance of habitat and competition. *J. Exp. Mar. Biol. Ecol.*, *75*, 119–127.
- Wissmar, R. C. and C. A. Simenstad. 1985. Surface foam chemistry and productivity in the Duckabush River estuary, Puget Sound, Washington, *in* *The Estuary as a Filter*, V. S. Kennedy, ed., Academic Press, 331–348.
- Woodin, S. A. 1985. Effects of defecation by arenicolid polychaete adults on spionid polychaete juveniles in field experiments: selective settlement or differential mortality. *J. Exp. Mar. Biol. Ecol.*, *87*, 119–132.